JOURNAL OF NEUROTRAUMA 33:917–928 (May 15, 2016)

DOI: 10.1089/neu.2015.4185

Serial Diffusion Tensor Imaging *In Vivo* Predicts Long-Term Functional Recovery and Histopathology in Rats following Different Severities of Spinal Cord Injury

Samir P. Patel,[1,2,*] Taylor D. Smith,[1,*] Jenna L. VanRooyen,[1,2] David Powell,[4,5] David H. Cox,[1] Patrick G. Sullivan,[1,3] and Alexander G. Rabchevsky[1,2]

Abstract

The current study demonstrates the feasibility of using serial magnetic resonance imaging (MRI) and diffusion tensor imaging (DTI) *in vivo* to quantify temporally spinal cord injury (SCI) pathology in adult female Sprague-Dawley rats that were scanned prior to a moderate or severe upper lumbar contusion SCI. Injured rats were behaviorally tested for hind limb locomotion (Basso, Beattie, Bresnahan [BBB] scores) weekly for 4 weeks and scanned immediately after each session, ending with terminal gait analyses prior to euthanasia. As a measure of tissue integrity, fractional anisotropy (FA) values were significantly lower throughout the spinal cord in both injury cohorts at all time-points examined versus pre-injury. Moreover, FA values were significantly lower following severe versus moderate SCI at all time-points, and FA values at the injury epicenters at all time-points were significantly correlated with both spared white and gray matter volumes, as well as lesion volumes. Critically, quantified FA values at subacute (24 h) and all subsequent time-points were highly predictive of terminal behavior, reflected in significant correlations with both weekly BBB scores and terminal gait parameters. Critically, the finding that clinically relevant subacute (24 h) FA values accurately predict long-term functional recovery may obviate long-term studies to assess the efficacy of therapeutics tested experimentally or clinically. In summary, this study demonstrates a reproducible serial MRI procedure to predict the long-term impact of contusion SCI on both behavior and histopathology using subacute DTI metrics obtained *in vivo* to accurately predict multiple terminal outcome measures, which can be particularly valuable when comparing experimental interventions.

Key words: anisotropy; BBB; contusion; gait analysis; magnetic resonance imaging (MRI); neuroimaging; white matter

Introduction

Clinical prognosis and classification of spinal cord injury (SCI) has relied primarily on the International Standards for the Neurological Classification of Spinal Cord Injury, as defined by the American Spinal Injury Association.[1] This assessment is based on neurological responses to sensory input as well as the strength of various muscles on both sides of the body. Notably, such physiological-based assessments can be confounded by the acute effects of spinal shock, namely neuronal hyperpolarization below the injury site, which can last up to 3 days post-injury, somewhat limiting the reliability of current standards for predicting functional outcomes.[2]

In animal models of SCI, the severity and classification of injury is traditionally assessed in terms of monitoring of various measures of functional recovery over time followed by terminal histopathology. While histology remains the premier method to assess the anatomy of the spinal cord after experimental SCI, the terminal nature of tissue processing is limiting. To assess tissue integrity at the injury site over time a different subject must be euthanized at each time-point to be evaluated.

Conventional magnetic resonance imaging (MRI) has been implemented to assess lesion volume in mice *ex vivo* following contusion SCI [3] and to assess neuroprotective effects of pharmaceutical compounds both *ex vivo* and *in vivo* in rats following SCI.[4,5] These studies utilized the measurement of changes in T2 relaxation times to identify tissue injury. Specifically, elevated T2 relaxation times within neuronal tissue often are reflective of cerebrospinal fluid (CSF)–filled lesion cavities, whereas shortened T2 relaxation times reflect hemorrhagic tissues. Threshold quantification methods used

[1]Spinal Cord and Brain Injury Research Center, [2]Department of Physiology, [3]Department of Anatomy and Neurobiology, [4]Magnetic Resonance Imaging and Spectroscopy Center, [5]Department of Biomedical Imaging, University of Kentucky, Lexington, Kentucky.
*These authors contributed equally to this study.

to assess T2 lesion volume typically indicate the presence of excess CSF or hemorrhage in otherwise healthy tissue; however, more sophisticated methods can provide much more information about the underlying microstructural integrity of the tissue being assessed.

Utilizing diffusion tensor imaging (DTI),[6] changes in tissue architecture and neuronal tract structure can be examined *in vivo* in terms of the selective preference of aqueous diffusion. Diffusion anisotropy calculated from DTI data, typically in terms of fractional anisotropy (FA), is a direct measure of the difference in the magnitude of diffusion in each direction and is a valuable metric by which to quantify anatomical microstructure.[7,8] Similarly, mean diffusivity is the average of the magnitude of diffusion in all dimensions. In the nervous system, this means that healthy white matter has relatively high FA (or more generally, diffusion anisotropy) due to the linear arrangement of myelinated axons, and low mean diffusivity for the same reason.[8] Critically, despite the nearly 15 years that DTI has been used to assess the spinal cord integrity *in vivo* in rodent models of SCI, these imaging studies have been performed largely *ex vivo*.[3,5,9–11]

In vivo DTI assessments as early as 1999 demonstrated location-dependent differences in various DTI metrics in the rat spinal cord, notably between gray and white matter.[12] This technique was then utilized to show decreased diffusion anisotropy and increased mean diffusivity in injured versus healthy spinal cords over time through serial acquisitions correlated with behavior (but not histology) in terms of hind limb locomotor assessments (Basso, Beattie, Bresnahan [BBB] scores), von Frey filament test, inclined plane, grid walk, and implementation of an activity box.[13,14] These studies, however, relied on invasive imaging techniques in which the receiver coil was implanted adjacent to the spinal cord. Kim and colleagues[15] adapted this technique to a truly non-invasive *in vivo* DTI protocol and also assessed changes in diffusion properties following a single severity of contusion SCI. In another study aimed at characterizing the progression of SCI from the acute through chronic phases, a longitudinal cross-sectional design was implemented to assess changes in T2 hyper-intensities, mean diffusivity, and diffusion anisotropy in the spinal cord from 2 through 25 weeks post-contusion SCI.[16] However, rather than acquire images in a serial manner, individual injury cohorts were utilized for each survival time-point and the DTI acquisitions for high-resolution assessment encompassing the entire injury site were acquired *ex vivo* en masse.[16]

While these studies provided crucial information indicating observable changes in the spinal cord following injury, the lack of different injury severities precluded information about the relationship of these changes with the degree of injury. Exclusively in the hyperacute phase (i.e., <6 h post-injury), *in vivo* DTI assessments have shown that decreased diffusion anisotropy and longitudinal diffusivity in the spinal cord are proportional to the injury severity, which was correlated with histological and behavioral outcome measures.[17–19] However, due to logistical and technical constraints, imaging during the hyperacute phase (< 6 h post-injury) for clinical assessments may not be practical. Since dynamics of the injury site from the hyperacute to the subacute phase (beyond 24 h post-injury) include a dramatic increase in the secondary damage cascade and cellular degeneration, an extension of this method beyond the hyperacute phase[15] while establishing both histological and behavioral correlations is unprecedented and warranted.

One of the crucial questions that have yet to be addressed is whether serial DTI acquisitions can accurately identify varying degrees of injury severity *in vivo* beyond the hyperacute phase, and whether changes in diffusion dynamics beyond the hyperacute phase precisely correlate with long-term behavioral outcome measures and terminal histology. Accordingly, the aim of these experiments was to establish a standard pragmatic method to perform serial DTI *in vivo* in adult rats for assessing tissue integrity over time following moderate and severe contusion SCI in order to predict multiple outcome measures of chronic functional recovery along with terminal histopathology.

Methods

Spinal cord injury

Female Sprague-Dawley rats ($n = 10$ total; Harlan Labs, Indianapolis, IN) weighing approximately 230 g were housed in the Biomedical and Biological Sciences Research Building animal facility at the University of Kentucky, and allowed *ad libitum* access to food and water. All animal procedures were approved by the Institutional Animal Care and Use Committee, University of Kentucky, and performed according to National Institutes of Health (NIH) guidelines. Animals were randomly assigned into two experimental groups prior to surgery in a manner such that on any given day, the experimenters were blinded to the experimental groups, which were equally numbered per injury cohort. Rats were anesthetized with ketamine (80 mg/kg; Fort Dodge Animal Health, Fort Dodge, IA) and xylazine (10 mg/kg, Lloyd Laboratories, Shenandoah, IA). A dorsal laminectomy of the 12th thoracic vertebra was performed to expose the 1st and 2nd lumbar spinal levels as described previously,[20] after which animals were subjected to a moderate (150 kDyn) or a severe (250 kDyn) spinal cord contusion injury using the Infinite Horizon impactor device (PSI, Lexington, KY).[21]

Immediately following injury, the wounds were irrigated with saline, the muscle layers were sutured together with 3-0 Vicryl (Ethicon, Inc., Somerville, NJ), and the skin closed together with surgical wound clips (Stoelting Co., Wood Dale, IL). Hydrogen peroxide and betadine were used to clean the surgical site and animals were injected subcutaneously with 10 mL pre-warmed lactated Ringer's solution (Baxter Healthcare Corporation, Deerfield, IL), Cefazolin (33.3 mg/kg; WG Critical Care, LLC, Paramus, NJ), and yohimbine (3.2 mg/kg; Lloyd Laboratorie) before being returned to their cages on a heating pad maintained at 37°C. Once rats regained consciousness, buprenorphine hydrochloride (0.03 mg/kg; Reckitt-Benckiser Pharmaceuticals Inc., Richmond, VA) was administered subcutaneously every 8 h for 72 h. Animals continued receiving cefazolin every 12 h through 5 days post-injury (DPI).

Behavioral assessment

The Basso, Beattie, Bresnahan Locomotor Rating Scale (BBB LRS)[22] was used to assess hind limb locomotor function of all rats. After pre-injury assessments, testing began at 2 DPI and continued weekly at 7 DPI through 28 DPI by individuals blinded to injury severity.

Additionally, at 28 DPI, all rats underwent gait analysis by recording from underneath using a high speed camera (Basler scA640; Basler AG, Highland, IL) while walking linearly across a transparent Plexiglas walkway. Step cycles were analyzed by demarcating when each foot was in contact with the Plexiglas frame by frame in order to determine the Regularity Index (RI), the Coordinated Pattern Index (CPI), and the Plantar Stepping Index (PSI), as we have described previously.[23]

MRI acquisition

Before and weekly after SCI, all rats underwent multi-parametric MRI scans in a 7T Clinscan MRI animal scanner (Bruker Biospin, Billerica, MA). Rats were anesthetized with 3% isoflurane and placed in the supine position on a heated bed with a constant ~2% isoflurane flow. A temperature probe and respiratory gating module were placed in order to monitor physiology throughout the scan. The L1/L2 spinal region was centered over a rat brain receiver coil

with a 2×2 array prior to inserting the bed into the scanner body. First, a localizer in the three orthogonal planes was used to verify the L1/L2 spinal level and determine slice positioning for subsequent scans. Next, a relaxometry multi-spin echo (MSE) sequence was run to acquire 14 slices over 9.8 mm spinal cord centered on the injury epicenter (field of view [FOV], 19 mm ×19 mm ×0.7 mm; matrix, 192×192×14 zero filled to 384×384×14) at multiple echo times in order to generate maps of proton density (PD) and T2 relaxation times (repetition time [TR] = 2000 msec; echo time [TE] = 23.1, 30.8, 38.5, …, 115.5, 123.2; number of sample averages = 5; total scan time, ~32 min). An echo-planar imaging DTI sequence was then acquired twice with two sets of six slices for a total of 12 slices spanning 9.6 mm centered on the injury epicenter (FOV, 17 mm ×23 mm ×0.8 mm; matrix, 96×128×6 zero filled to 192×256×6) from which the FA images were derived (TR = 1700 msec; TE = 32 msec; b = 0, 800; number of b_0 scans = 10; number of diffusion encoded scans = 96; number of sample averages = 4; total scan time = ~24 min [12 min ×2]). The same acquisitions were completed prior to injury and at 7 DPI, 14 DPI, 21 DPI, and 28 DPI.

MRI analysis

All MRI post-processing, unless otherwise stated, was completed using the FSL FMRIB Software Library v5.0 (Analysis Group; FMRIB, Oxford, UK).[24] PD and T2 maps were generated from multi-spin echo (MSE) acquisitions by fitting the intensity for each voxel over time to the T2 decay curve $I_t = I_0 e^{-t/T2}$ using the Analysis of Functional NeuroImages MRI analysis suite (National Institute of Mental Health, Bethesda, MD), where I_t is the intensity at time t, I_0 is the initial intensity (or the PD), t is the time in milliseconds, and $T2$ is the T2 relaxation time for the given subvolume. These reconstructed maps were utilized in place of single PD-weighted or T2-weighted images in order to nullify the effects of variable signal intensity at different distances from the coil. The spinal cord was then demarcated from the T2 map by manually overlaying a user generated mask (Fig. 1). Masks were generated using PD images as a reference, due to their enhanced morphometric clarity. For each cord, the mean and standard deviation of the T2 parameter throughout the entire cord (including the injury) was calculated and a threshold applied such that any voxel with a value greater than 3 standard deviations (SD) above the cord mean was considered T2 hyper-intense, where the total volume of T2 hyper-intense voxels within a subject represents the T2 lesion volume. The T2 maps demonstrated negligible T2 hypo-intensities; therefore, they were excluded from quantification of T2 lesion volume. A threshold of 3 SD was chosen by experimentation, as it yielded the greatest noise reduction without additionally excluding appropriately T2 hyper-intense regions. When 2 SD was applied, it resulted in increased noise that could have classified healthy tissue as T2 hyper-intense. On the other hand, 5 SD resulted in virtually no T2 hyper-intensities. The same was done for hypo-intense regions with low T2-relaxation times; however, there was negligible detection with this method.

Finally, inclusion or exclusion of the injury site (epicenter) for this threshold determination did not affect determination of T2 lesion volumes, as any arbitrary threshold value chosen was effectively either too low so as to include noise or too high so as to exclude clearly pathological tissue. The generated masks also were used to calculate cord volume on a slice-by-slice basis in order to assess spinal cord atrophy over time. FA maps were generated inline on the Clinscan using the Syngo MR Software suite (Syngo MR B17; Siemens AG, Erlangen, Germany). The captured spinal cord slice images were then extracted using a manually generated mask (Fig. 1) and the average cross-sectional FA was determined for each slice, as well as averaged for the entire spinal cord.

Histology

Following 28 DPI behavioral assessments and MRI, animals were transcardially perfused with 4% paraformaldehyde (PFA) in 0.1 M

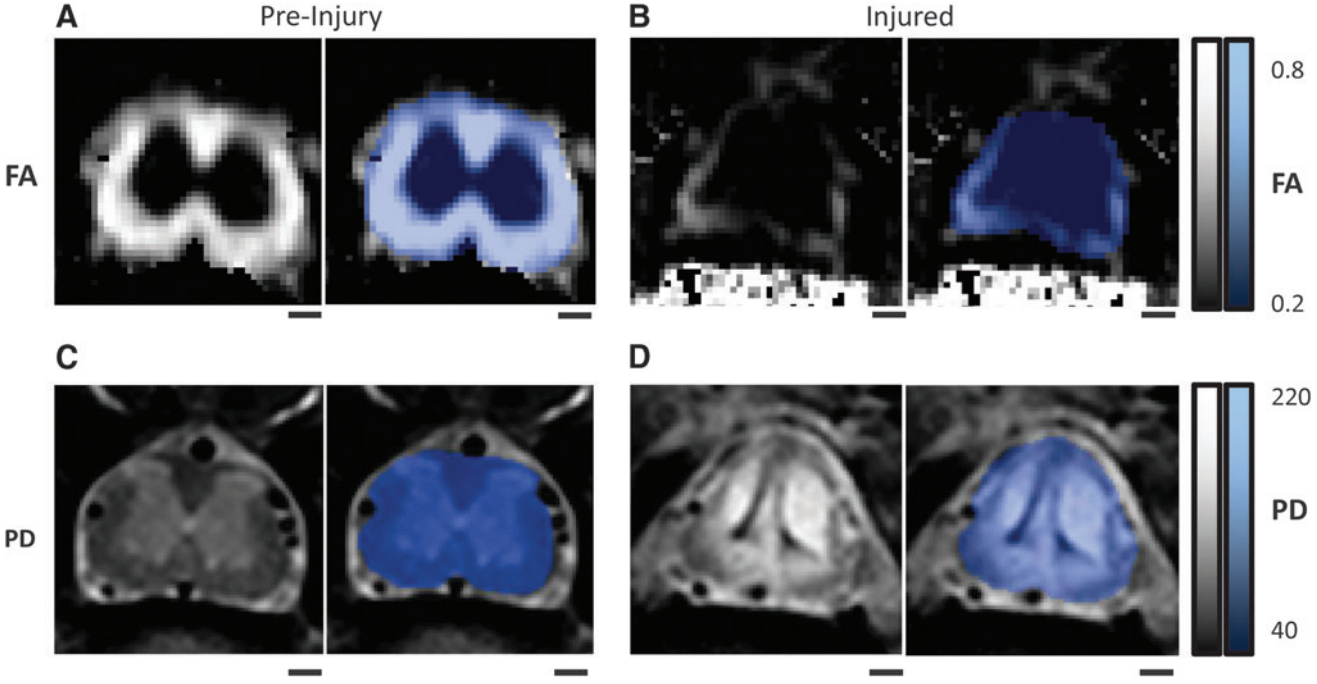

FIG. 1. Fractional anisotropy (FA; **A** and **B**) and complementary proton density (PD; **C** and **D**) images for a single rat captured pre-injury (A, C) and at 28 days post-injury (B,D) at the same L1/L2 spinal level, with associated spinal masks (blue). The spinal cord masks (blue) are applied after image acquisition to specifically analyze only spinal tissue and not surrounding tissues. Lighter color for FA is indicative of more anisotropic flow, whereas brighter color in the PD is indicative of higher proton concentration. Scale bars = 500 μm. Color image is available online at www.liebertpub.com/neu

phosphate-buffered saline (PBS). To maintain consistent sampling, each spinal cord from the L1/L2 injury cohorts was transected at the rostral T11 spinal root and a 30-mm spinal cord segment was immediately dissected and post-fixed for 2–4 h in 4% PFA/PBS at 4°C. This was followed by overnight washing with 0.1 M PBS at 4°C before cryo-protecting in 20% sucrose/PBS at 4°C and embedding tissues as we have described.[25] Frozen spinal cords were then serially cryo-sectioned at 20 μm and subjected to eriochrome cyanine staining to differentiate white matter and gray matter.[25,26]

The lesion volume and volume of spared tissues were calculated using a modified Cavalieri method from a series of seven evenly-spaced sections (1 mm apart) centered at the injury epicenter in order to represent the length of spinal cord used for MRI analysis (a series of nine evenly-spaced slices, 0.8 mm apart, 7.2 mm total centered on injury site). As we have detailed previously, for each 20 μm spinal cord cross-section, the area of lesion, spared gray matter, and spared white matter were quantified, and the respective sub-volumes within the assessed cords were determined by summation, in addition to quantifying tissue sparing at the injury epicenter.[20,25] As we have reported, spared tissue was identified by positive staining of myelin in white matter and the cyto-architecture of gray matter representative in naïve animals, whereas lesions were identified as regions lacking normal characteristic traits.[27] All morphometric quantifications were completed using a Nikon microscope (Nikon Corporation, Tokyo, Japan) and Scion imaging analysis software (Scion Corporation, Frederick, MD).

Statistical analysis

Long-term BBB LRS was analyzed using a repeated measure analysis of variance (ANOVA) with Holm-Sidak *post hoc* analysis when warranted, while histological and gate assessments were analyzed by one-tailed unpaired t-tests using GraphPad Prism 6 (GraphPad Software, Inc., La Jolla, CA). FA throughout the rostrocaudal spinal cord were analyzed relative to time, spinal level, and injury severity using repeated measures ANOVA with one between subject factor (injury) and two within subject factors (time and spinal level) with Fisher's LSD *post hoc* analysis in the SAS software suite (SAS Institute Inc., Cary, NC). For all data analysis, significance was set at $p < 0.05$.

Results

Following pre-injury scanning, animals received a contusion SCI. Injury parameters were comparable to our previous reports for force (moderate, 154.8 ± 2.2 kDyn; severe, 283.8 ± 22.9 kDyn), displacement (moderate, 996.0 ± 39.8 μm; severe, 1541.0 ± 41.9 μm), and velocity (moderate, 124.3 ± 1.0 mm/sec; severe, 121.8 ± 2.3 mm/sec).[21,23,27] One animal from the moderate injury cohort was excluded from further analysis due to poor tissue fixation resulting in unquantifiable histology.

Effect of injury severity on functional recovery

Hind limb locomotor recovery was assessed prior to injury, as well as at 2, 7, 14, 21, and 28 DPI.[22] Gross hind limb locomotor recovery patterns were consistent with our previous reports showing immediate deficits following different injury severities with differential recovery thereafter.[21,23,27] Two-way ANOVA revealed significant effects of injury severity ($F[1,7] = 12.02$; $p = 0.01$) and time ($F[5,35] = 40.71$; $p < 0.0001$) with a significant interaction ($F[5,35] = 2.711$; $p = 0.04$; Fig. 2). Holm-Sidak *post hoc* analysis revealed significant group differences at 2 and 28 DPI. The moderate SCI group demonstrated mild paralysis acutely after injury, whereas the severe SCI group showed complete paralysis. Overall, by 28 DPI, the rats in the moderate SCI group exhibited consistent plantar stepping and consistent forelimb-hind limb (FL-HL) coordination, with consistent toe clearance during forward limb advancement, reflected in a BBB score of ~18. On the contrary, the severe SCI group regained only occasional to frequent weight-supported plantar stepping without FL-HL coordination, reflected in a BBB score of ~10.

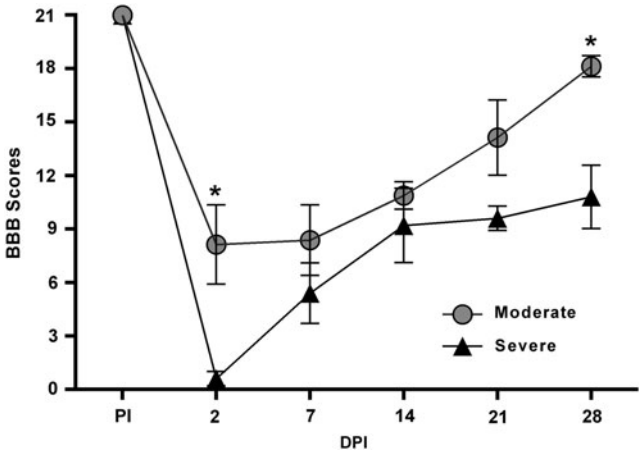

FIG. 2. Loss and recovery of hind limb function following moderate and severe contusion spinal cord injury (SCI). Graphic representation of the mean behavioral (Basso, Beattie, Bresnahan [BBB]) scores pre-injury (PI) and at 2, 7, 14, 21, and 28 days post-injury (DPI). At 2 DPI, rats with moderate SCI had only partial paralysis with prominent hind limb movements, compared with complete paralysis seen in rats with severe SCI. Rats with moderate SCI further showed significantly improved recovery of hind limb locomotion over time, compared with severe SCI. Symbols represent group means ± standard error of the mean, $n = 4$–5/group. *$p < 0.005$, compared with severe SCI.

As a more refined measure of locomotor function, terminal gait assessments were performed in order to calculate the percentages of the CPI (FL–HL coordination and dorsal stepping), the PSI (fidelity of plantar stepping), and the RI (mirrors CPI, does not

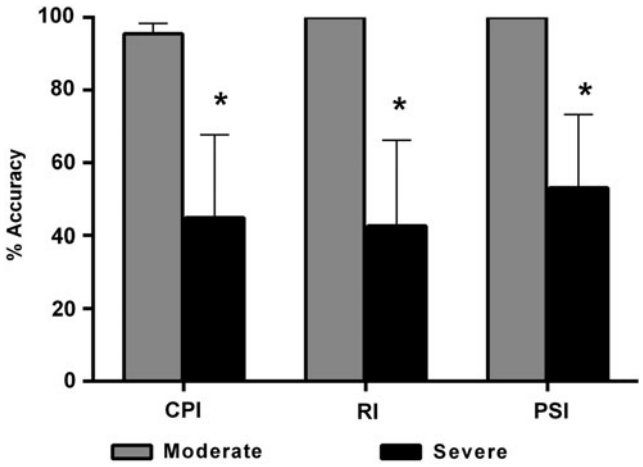

FIG. 3. Terminal gait analyses at 28 days following moderate or severe contusion spinal cord injury (SCI). Comparisons of Coordinated Pattern Index (CPI), Regularity Index (RI) and Plantar Stepping Index (PSI). Rats in the severe SCI group showed significantly lower % CPI, % RI and % PSI at 28 DPI, compared with moderate SCI. Bars represent group means ± standard error of the mean, $n = 4$-5/group. *$p < 0.05$, compared with moderate SCI.

incorporate dorsal stepping and is not sensitive to double stepping; Fig. 3). Unpaired Student's *t*-test showed that % CPI ($p = 0.046$), % RI ($p = 0.03$), and % PSI ($p = 0.04$) were significantly higher in the moderate versus severe SCI group. The moderate SCI group also demonstrated exceptional recovery, with no dorsal stepping and perfect RI footfall pattern coordination, with occasional double-stepping as reflected in the slight deficit in % CPI. The severe SCI group had considerably less coordination as reflected in ~45% reductions of % CPI and % RI, with dorsal stepping of the hind limbs.

Effect of injury severity on MRI-based morphometrics

PD and T2 maps were generated from the spin-echo sequence (see Methods). The PD images provided exceptional clarity in healthy tissue, allowing differentiation of white matter, gray matter, CSF, and bone (Fig. 1). However, the distinction between spared or injured tissues was not clearly distinguishable within individual cross-sections, precluding accurate manual segmentation of injured and spared tissue. At 7 DPI, the epicenter and adjacent slices were almost completely homogeneous for both cohorts, with little to no distinction between white matter, gray matter, and lesion (not shown). At this point in time, the only notable difference between the injury cohorts was a narrow band of spared white matter in the moderate SCI group along the ventrolateral spinal cord. By the terminal time-point, however, differences between moderate and severe contusions were clear (Fig. 4). Invariably, PD maps of the injury epicenter for the moderate injuries contained two signal hypo-intense regions on either side of the central canal, accompanied by a hyper-intense region encompassing the dorsal columns (Fig. 4A). These spinal cords showed distinct spared white matter in the ventrolateral funiculi and the superficial dorsal horns, often remaining conspicuously visible. The cords also appeared slightly compressed along the dorsal-ventral axis.

Alternatively, in the severe SCI group, maps of PD demonstrated greater homogeneity throughout the lesion site, similar to the earlier time-points after moderate SCI. There were similar PD hypo-intense regions lateral to the central canal; however they were smaller and much less distinct than those present in the moderate SCI group, while the PD hyper-intense regions were dispersed

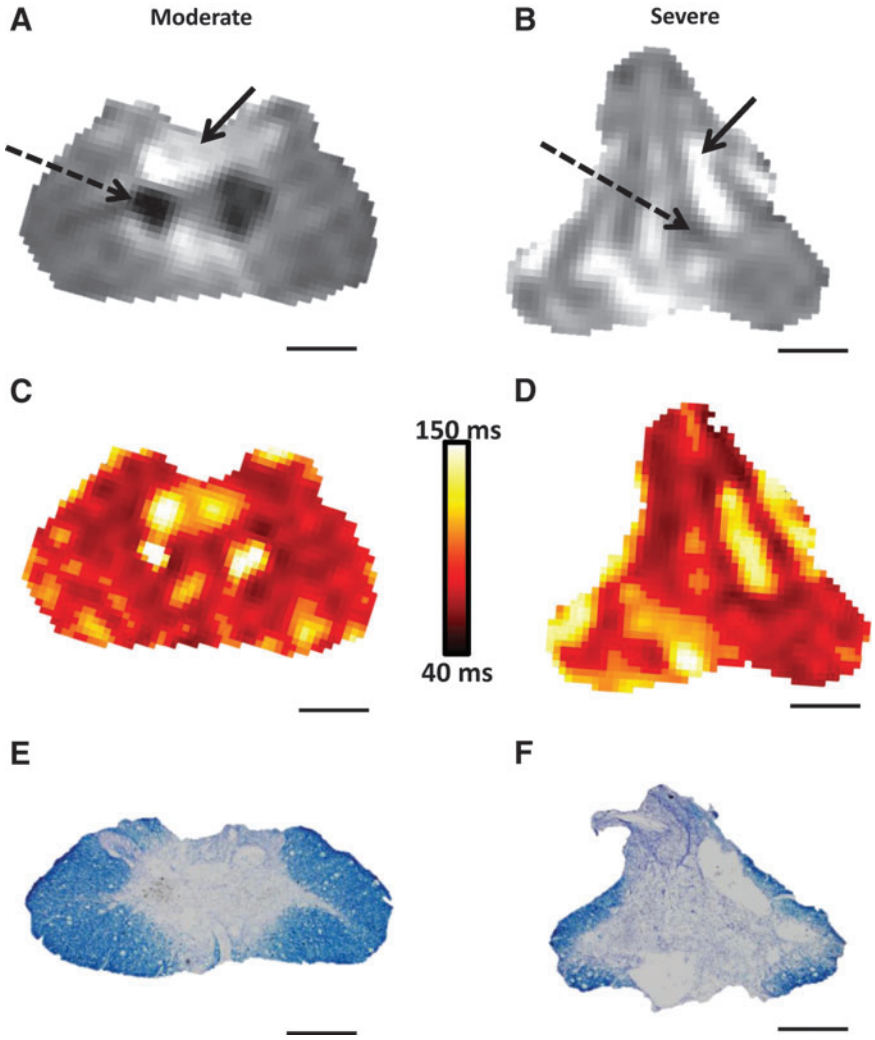

FIG. 4. Photomicrographs of representative proton density images 28 days after moderate and severe spinal cord injury (SCI; **A, B**) along with corresponding maps of T2 relaxation times *in vivo* (**C, D**) and histological (eriochrome cyanine–stained) sections *in situ* (**E, F**). Note that dashed arrows indicate regions with little tissue density while solid arrows indicate high intensity regions indicative of fluid filled lesion cavities. Scale bars = 500 μm. Color image is available online at www.liebertpub.com/neu

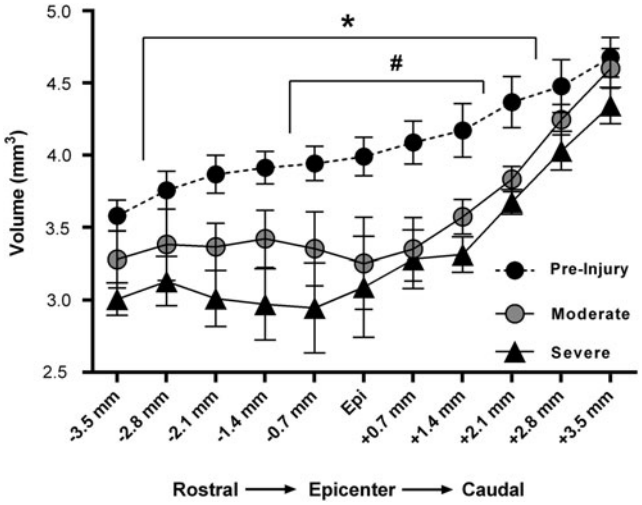

FIG. 5. Graphical representation of in-vivo magnetic resonance imaging–derived cross-sectional subvolumes throughout the spinal cord at 28 days post-contusion spinal cord injury (SCI), compared with pre-injury volume. Compared with pre-injury volumes, severe SCI resulted in significantly decreased subvolumes extending from 2.8 mm rostral to 2.1 mm caudal to the injury epicenter, whereas moderate SCI resulted in significantly decreased subvolumes extending only from 0.7 mm rostral to 1.4 mm caudal to the injury epicenter. $*p < 0.05$ severe SCI, compared with pre-injury. $\#p < 0.05$ moderate SCI, compared with pre-injury.

throughout the cross-section (Fig. 4B). The more severe injury also resulted in a consistent dorsal-ventral elongation of the spinal cord with apparent atrophy of the lateral funiculi. Note that while some of the major features of the injury are visible in the brilliant T2 images (Fig. 4C, 4D), they contain far more noise than the associated PD images. Total cord volume significantly decreased over time following SCI ($F[4,28] = 13.83$; $p < 0.0001$); however, there was no significant effect of injury severity. Both injury cohorts showed a trend of lower cord volumes at 14, 21, and 28 DPI ($p > 0.05$), compared with pre-injury volumes; however, severe SCI resulted in significantly decreased volume at 21 and 28 DPI, compared with 7 DPI (data not shown).

As an assessment of the terminal change in spinal cord volume, the terminal volume of each slice for both groups was compared with their associated, statistically indistinguishable, combined pre-injury volumes. Compared with pre-injury cord volumes, there was a significant effect of spinal level ($F[10,150] = 72.17$; $p < 0.0001$) and injury ($F[2,15] = 6.01$; $p = 0.012$) with a significant interaction ($F[20,150] = 2.95$; $p < 0.0001$) at 28 DPI (Fig. 5). *Post hoc* analysis revealed that, compared with pre-injury cord volumes, moderate SCI resulted in a significantly lower subvolume (i.e., slice) at the injury epicenter, as well as one slice rostral and two slices caudal. Alternatively, severe SCI resulted in significantly lower subvolumes in all slices except those farthest rostral and caudal from the injury epicenter, indicating significantly greater spinal cord atrophy. However, quantitative assessment of T2 maps did not show any significant changes in T2 hyper-intense lesion volume over time (Fig. 6A), nor were there any significant differences between injury groups throughout the rostro-caudal extent at the terminal time-point (Fig. 6B). Note that while there was a trend for higher T2 lesion volumes after moderate versus severe SCI at both 7 and 14 DPI, quantitative comparisons of T2 lesion volumes between injury severities were inconclusive based on the high variability.

Effect of injury severity on histopathology

In accordance with terminal MRI imaging (Fig. 4A, 4B), qualitative histology revealed conspicuously greater lesion area and reduced tissue sparing at the injury epicenters following severe versus moderate SCI (Fig. 4C, 4D), which was confirmed by injury morphometric analysis between the groups (Fig. 7). An unpaired *t*-test showed that moderate SCI resulted in significantly lower lesion volume, compared with the severe SCI group (Fig. 7A). Two-way ANOVA indicated a significant effect of injury severity ($F[1,7] = 17.56$; $p = 0.004$) and spinal level ($F[10,70] = 25.63$; $p < 0.0001$) on lesion volume with a significant interaction ($F[10,70] = 2.54$; $p = 0.01$). *Post hoc* analysis revealed significant differences in lesion subvolumes across equally spaced tissue sections (Fig. 7B), with the moderate SCI group showing greater tissue sparing at the

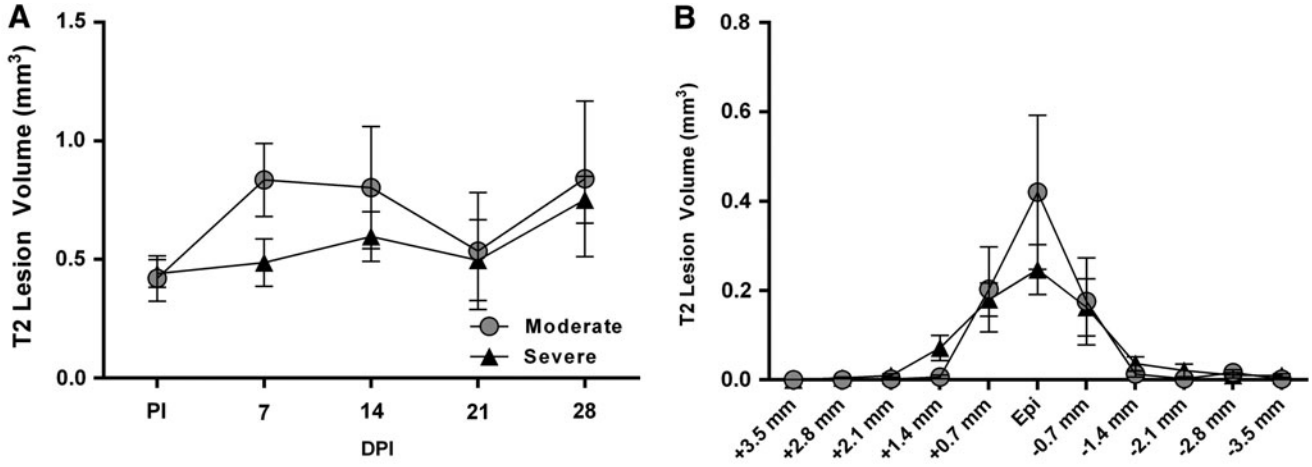

FIG. 6. **(A)** Graphical illustration of total T2 lesion volumes comprising 8.8 mm of spinal cord analyzed for each rat in both injury cohorts beginning at 7 and continuing to 28 days post-injury (DPI). There were no significant group differences and no significant changes within groups over time. **(B)** Depiction of T2 lesion subvolumes throughout the cord for both injury cohorts at 28 DPI. Symbols represent group means ± standard error of the mean. PI, pre-injury; epi, epicenter.

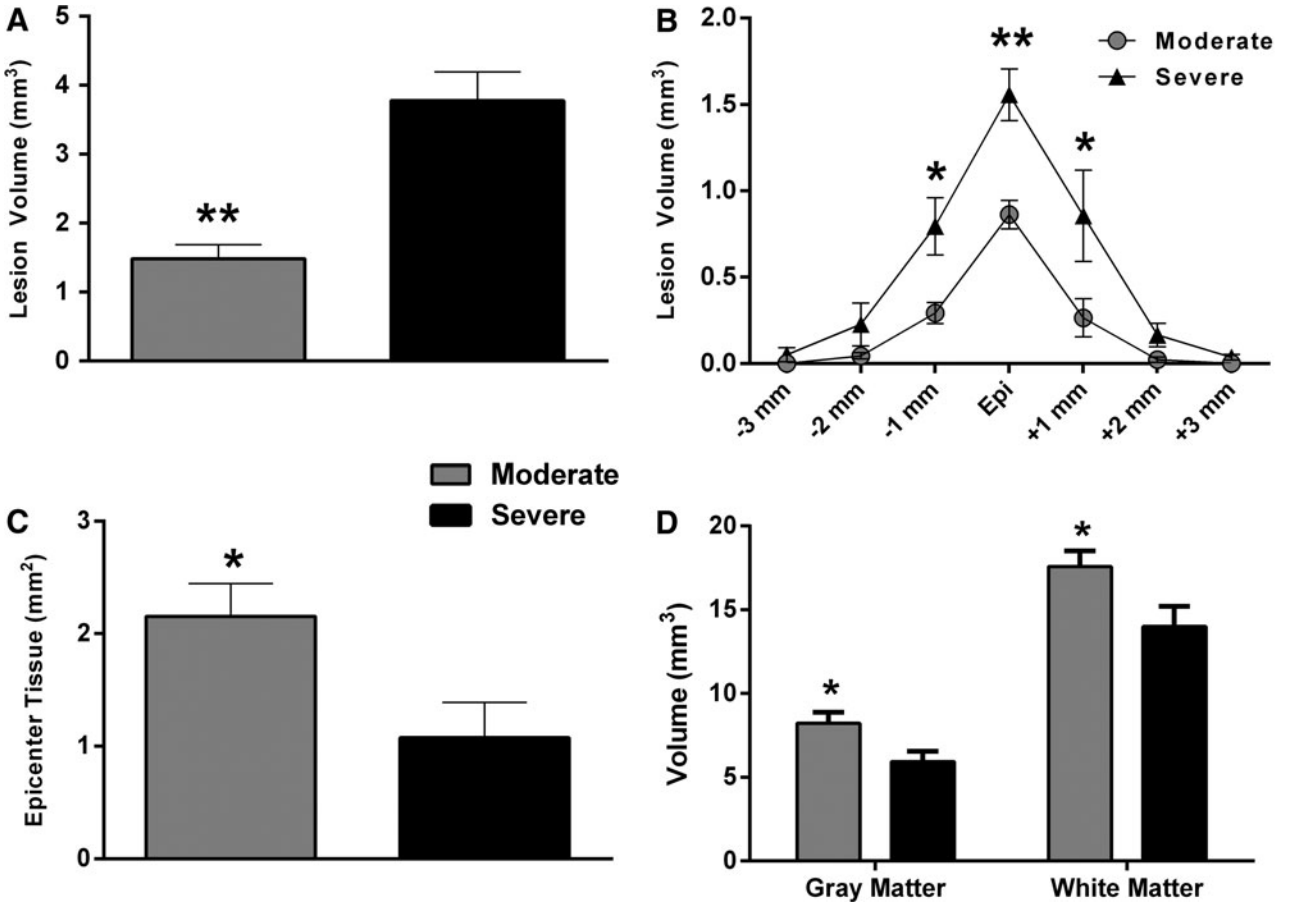

FIG. 7. **(A)** Lesion volume was significantly greater in the severe spinal cord injury (SCI) cohort. **(B)** Throughout the rostro-caudal extent of the injured spinal cords, differences in lesion subvolumes were greatest at the injury epicenters (Epi) and significantly higher in the moderate SCI cohort, compared with the severe SCI cohort **(C).** Spared gray matter and white matter volumes throughout the injured spinal tissues were significantly higher after moderate, compared with severe SCI **(D).** Bars/symbols represent group means ± standard error of the mean, $n = 4$-5/group. $^{*}p < 0.05$; $^{**}p < 0.01$, compared with severe SCI.

injury epicenter, compared with severe SCI (Fig. 7C). Moreover, the volume of spared gray matter and white matter throughout the spinal cord were significantly lower after severe versus moderate SCI (Fig. 7D).

Effect of injury severity on cross-sectional FA at injury epicenter

User-generated masks were overlaid on FA images in order to exclusively assess spinal cord tissue. Pre-injury FA values were virtually identical for each evenly-spaced spinal cord slice (0.8 mm thick) between the injury groups (Fig. 8). A two-way ANOVA revealed main effects of injury severity ($F[1,7] = 37.87$; $p = 0.0005$) and spinal level ($F[4,28] = 95.45$; $p < 0.0001$) with a significant interaction ($F[4,28] = 3.726$; $p = 0.01$). *Post hoc* analysis showed that, irrespective of injury severity, the average slice FA at the injury epicenter at all four time-points were significantly lower, compared with pre-injury. Further, FA at the injury epicenter was significantly lower in the severe SCI group than the moderate SCI group at all four time-points post-injury, with increased group separation over time. In contrast to stable FA values for the moderate SCI group over time following injury, the severe SCI group showed a trend for decreased FA over time following SCI.

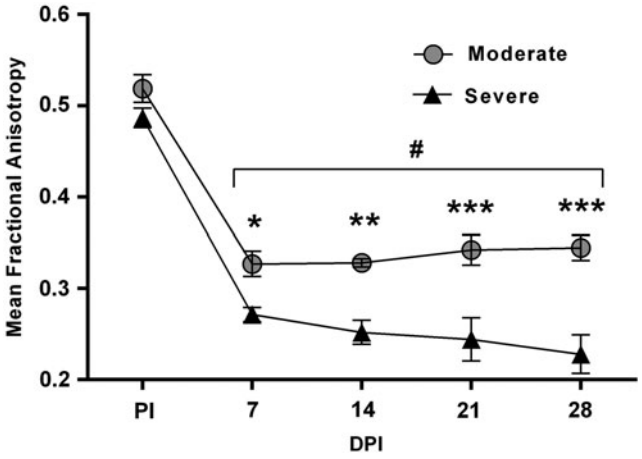

FIG. 8. Comparison of mean fractional anisotropy (FA) at the injury epicenter (L1/L2 spinal levels) in moderate versus severe spinal cord injury (SCI) prior to injury (PI) and at 7, 14, 21, and 28 days post-injury (DPI). Severe SCI significantly decreased FA, compared with moderate SCI at all time-points assessed, starting as early as 7 DPI. Symbols represent group means ± standard error of the mean. $\#p < 0.0001$, compared with PI; $^{*}p < 0.05$, $^{**}p < 0.005$, $^{***}p < 0.0001$, compared with severe SCI.

Effect of injury severity on cross-sectional FA throughout the rostro-caudal spinal cord

Analysis of FA at all spinal levels over time was performed with a repeated measures ANOVA, revealing significant effects of time ($F[4,28] = 45.53$; $p < 0.0001$), injury severity ($F[1,7] = 46.65$; $p = 0.0002$), and spinal level ($F[8,56] = 123.86$; $p < 0.0001$), with a significant interaction ($F[32,224] = 2.16$; $p = 0.0006$; Fig. 9). *Post hoc* analysis revealed that, compared with pre-injury FA values, contusion SCI resulted in significantly lower FA for each spinal cord level assessed at all four time-points, independent of injury severity. Notably, there were no significant changes in FA over time for both injury cohort between 7 and 28 DPI.

FA is predictive of long-term locomotor recovery

Correlation analyses showed that the terminal BBB scores were significantly correlated with injury epicenter FA values at 7 ($r = 0.808$; $p = 0.008$) and 28 DPI ($r = 0.775$; $p = 0.014$; Fig. 10A, 10B). Importantly, the significant correlation between epicenter FA at 7 DPI and terminal BBB scores indicate the prognostic value of MRI-DTI to predict long-term functional recovery. Similarly, terminal % CPI was significantly correlated with epicenter FA at 7 ($r = 0.707$; $p = 0.033$) and 28 DPI ($r = 0.657$; $p = 0.047$; Fig. 10C, 10D), as were RI and PSI metrics (data not shown). Similar to the significant predictive correlations with BBB, this shows the capacity of early FA values to accurately predict long-term recovery of more refined motor control.

FA is predictive of terminal histopathology

Irrespective of injury severity, histological measures were highly correlated with injury epicenter FA values at 7 and 28 DPI (Fig. 11). There were significant correlations between FA values at 7 DPI and terminal histopathology in relation to lesion volume (Fig. 11A;

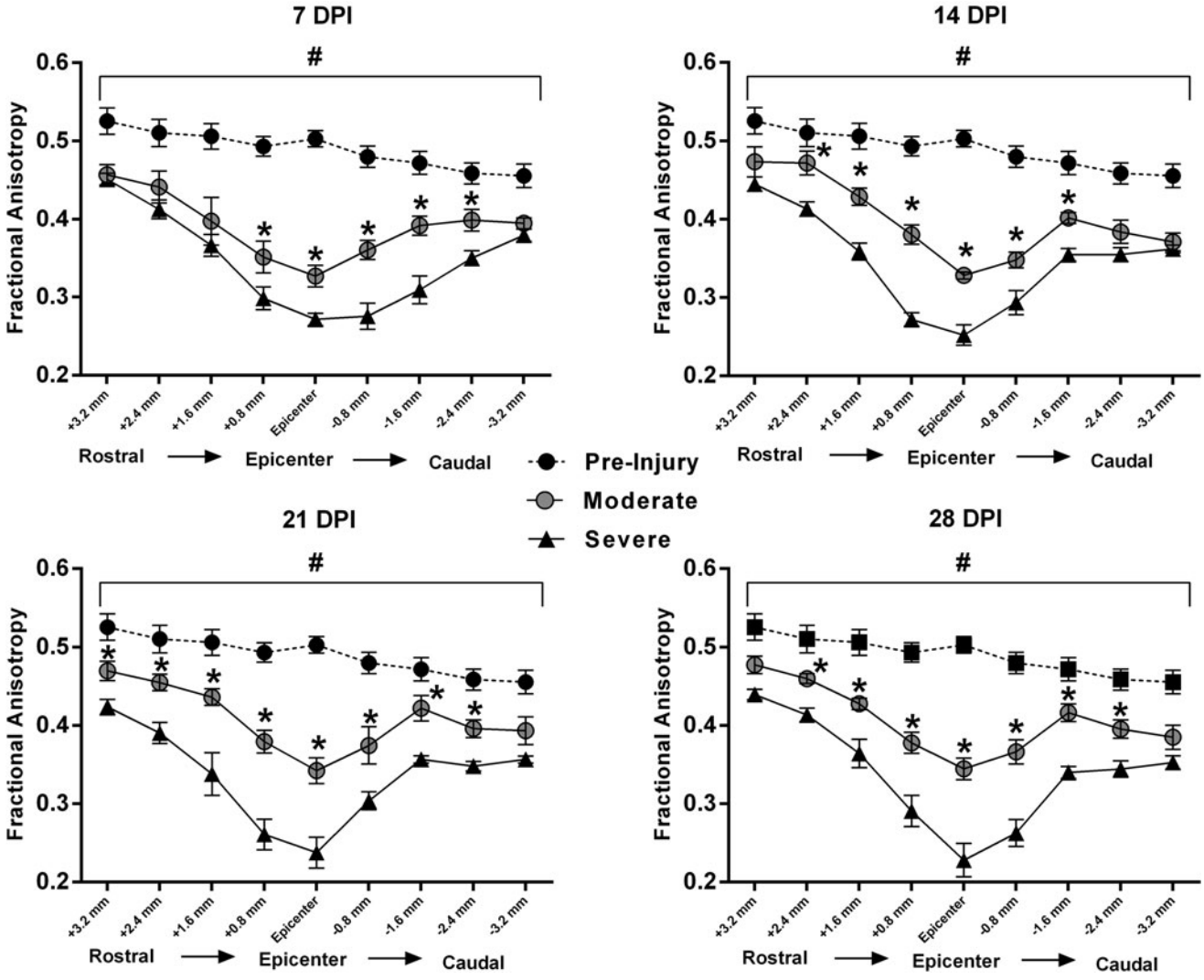

FIG. 9. Graphical representations of average cross-sectional fractional anisotropy (FA) values of nine evenly-spaced DTI slices (0.8 mm thick) centered at the injury epicenter. Compared with pre-injury FA values, both injury severity cohorts had significantly lower FA at all spinal levels, at all four time-points. At 7 days post-injury (DPI), there was an initial separation between moderate and severe SCI groups more prominent caudal to the injury epicenter. At 14, 21, and 28 DPI, FA values were significantly lower for all the adjacent slices in the severe SCI group, compared with the moderate SCI group, excluding the farthest rostrocaudal slices. Symbols represent group means ± standard error of the mean, $n = 9$ for pre-injury and $n = 4$-5/group for moderate and severe. #$p < 0.05$, compared with both moderate and severe SCI; *$p < 0.05$, compared with severe SCI.

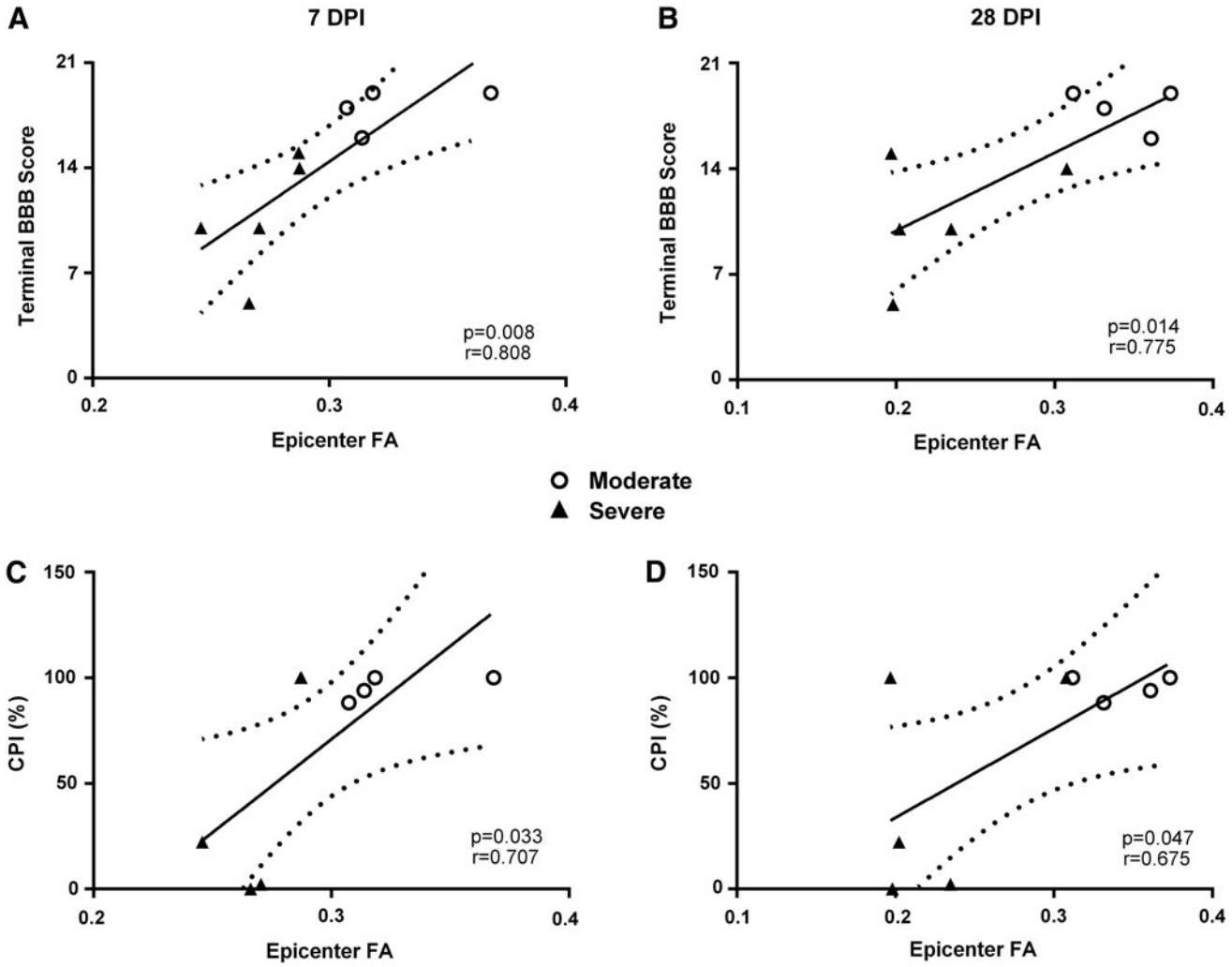

FIG. 10. Correlations between fractional anisotropy (FA) at the injury epicenters and behavioral metrics over days post-injury (DPI). At both 7 and 28 DPI, FA values were significantly correlated with terminal Basso, Beattie, Bresnahan (BBB) scores **(A, B)** and % Coordinated Pattern Index (CPI; **C, D).** Open circles represent rats with moderate SCI and black triangles represent those with severe SCI. Solid line represents line of best fit; dotted lines represent 95% confidence interval.

$r=0.896$; $p=0.001$), epicenter tissue sparing (Fig. 11B; $r=0.857$, $p=0.003$), spared white matter volume (Fig. 11C; $r=0.750$; $p=0.02$), and spared gray matter volume (Fig. 11D; $r=0.783$; $p=0.02$). As anticipated, similar correlations were observed with 28 DPI FA values (Fig. 11E-H). This demonstrates that FA values at subacute timepoints post-injury are highly predictive of the neuroanatomical integrity of residual white matter and gray matter tissues weeks following SCI.

Discussion

The present study used serial MRI *in vivo* to temporally assess the pathophysiology following different severities of contusion SCI by quantifying various MRI-based outcome measures that reflect distinct aspects of tissue integrity. While T2 mapping was suitable to identify and localize the injury, we found it was not capable of accurately quantifying the volume of either injured or spared tissue over time post-injury, notably in terms of signal hyper-intensity/hypo-intensity. Lesion volume calculations based on measuring T2 hyper-intense regions *in vivo* were inconclusive and showed no correlations with behavioral or histological measures. This effect was much more pronounced for the severe SCI cohort, where discrete foci of T2 hyper-intensity/hypo-intensity were rarely observed. DTI, on the other hand, provided much more compelling results directly related to the injury severity. In particular, DTI-derived FA values were decreased at the injury epicenter and in penumbral spinal tissues relative to pre-injury levels, and the decrease in FA values was proportional to the injury severity. Most critically, DTI (FA) assessments were significantly correlated with- and highly predictive of- injury severity-dependent functional recovery, as well as morphometric histopathology.

Prior to injury, cross-sectional spinal cord FA was effectively equal between groups, with a steady but marginal decrease in cross-sectional FA progressing rostral to caudal. Since white matter is inherently more anisotropic than gray matter, this decrease is likely due to the lower ratio of white to gray matter in more caudal segments. Our study demonstrated a significant decrease in average cross-sectional FA values at all spinal levels measured *in vivo* following SCI in both injury groups, compared with pre-injury levels. While there were no apparent changes in FA values over

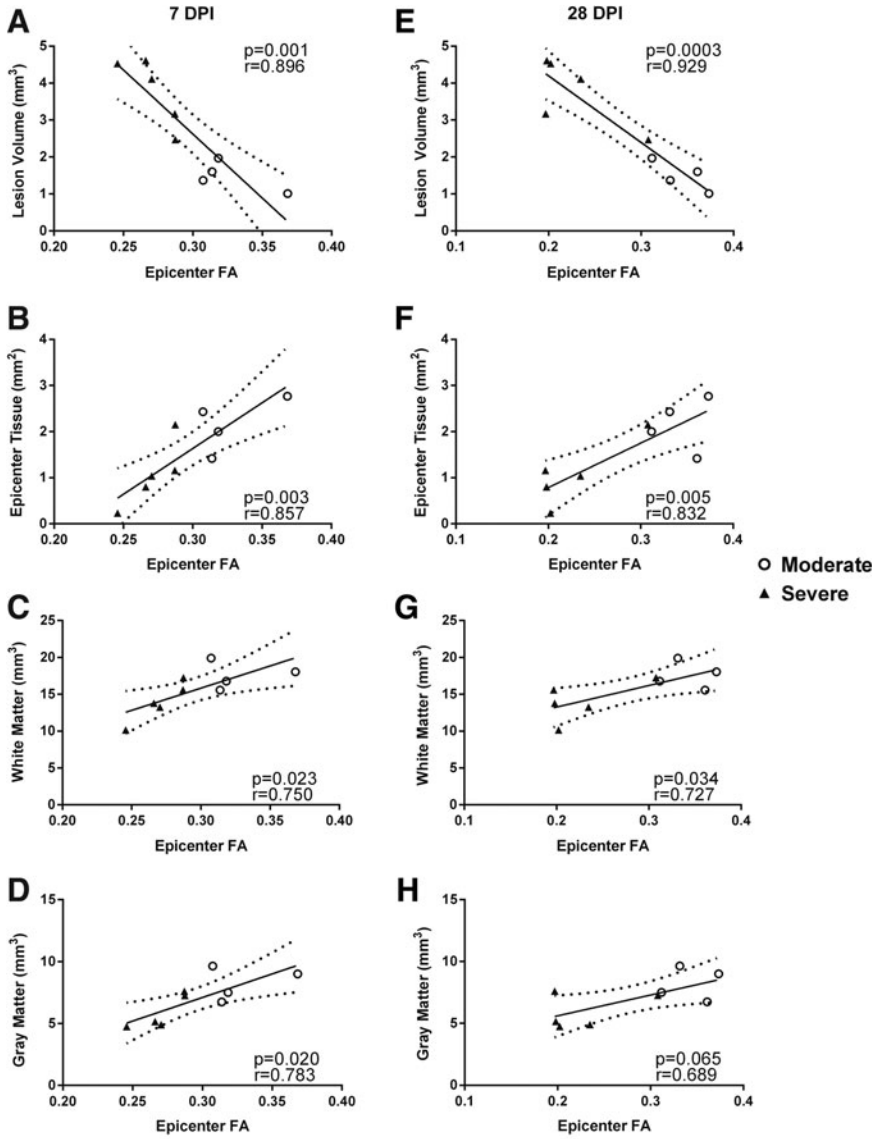

FIG. 11. Correlation analyses of fractional anisotropy (FA) at the injury epicenters at 7 and 28 days post-injury (DPI) with various histological measurements. FA at 7 DPI was significantly correlated with terminal histology in terms of lesion volume **(A),** epicenter tissue sparing **(B),** white matter volume **(C)** and gray matter volume **(D).** FA at 28 DPI was also significantly correlated with each of these same metrics, except for gray matter volume **(E-H).** Open circles represent rats with moderate spinal cord injury (SCI) and black triangles represent those with severe SCI. Solid line represents line of best fit; dotted lines represent 95% confidence interval.

time following moderate SCI, the severe SCI group showed a comparatively insignificant trend towards decreasing FA values over time post-injury. In spite of the static FA values following injury, both the moderate and severe SCI groups showed improved functional recovery (BBB scores) over time, consistent with our previous report that functional recovery following SCI is dependent on the amount of spared tissue at acute time-points after injury[25].

The FA throughout each cross-section including both the gray and white matter was averaged in an effort to develop a procedure with a single discrete output parameter of tissue integrity while maintaining a high level of consistency. Despite the relatively isotropic nature of gray matter, compared with white matter, it has been shown that FA is markedly reduced in both gray and white matter following contusive SCI in rats.[10] As such, the FA for each entire cross-section was averaged in order to effectively assess the global level of microstructural degradation. Moreover, rather than assess individual cellular components potentially responsible for changes in FA (such as axonal collapse or myelin swelling), the stereological assessments were restricted to volumes of lesion and spared tissues.

It is also worth noting that the relatively small sample size for the current study speaks to the strengths of the methodologies employed due to the substantial and consistent significant effects observed; however, the resulting decrease in the power of correlational analyses cannot be overlooked. Moreover, aside from increasing the sample size for each of the cohorts, inclusion of an additional minor injury group may have lent more power to this study. Given technical and logistical considerations regarding MRI scanning times and scanner availability, such inclusion was not possible for the current study.

There have been a number of studies in uninjured humans and other animal species to assess spinal cord morphology and structure using MRI and DTI.[8,28,29] Various DTI metrics, including FA, have been shown to be significantly different between regions of gray matter and white matter, yet FA values remain relatively equal throughout white matter or gray matter, respectively.[28,29] Increased FA in the white matter relative to gray matter is theorized to be due to arrangement of myelinated axons in the direction of the longitudinal spinal cord axis, thus inhibiting diffusion in the transverse direction.[8]

Clinically, MRI is used in SCI almost exclusively for preoperative neurosurgical planning, primarily providing insight into the gross morphometry of the injury site.[30,31] In humans with chronic thoracic SCI, MRI-DTI has shown decreases in diffusion anisotropy (one dimensional) in cervical white matter, compared with uninjured subjects.[32] While this demonstrated potential diagnostic and prognostic use of DTI to classify chronic SCI, it could not provide insight into the progression of the measured parameters over time. MRI studies in rats *ex vivo* have documented that FA is decreased in both white matter and gray matter following contusion SCI, with particular detriment at the injury epicenter.[9,10] These studies provided critical information proximal to the injury site, but the *ex vivo* post-mortem nature of the MRI assessments employed is not practical since critical information can be obtained with higher fidelity using considerably more resolute histology.

Accordingly, a more recent study that used *in vivo* MRI-DTI to assess SCI pathology over time demonstrate significantly decreased FA values in rats after SCI versus controls at both the injury epicenter, as well as in penumbral tissues.[33] The short time scale of this experiment (scanning <6 h post-injury), however, did not allow for evaluation of temporal differences in DTI metrics such as FA. Another study assessing DTI metrics following moderately severe contusion SCI in rats showed significant correlations between terminal (56 DPI) DTI metrics and terminal behavioral assessments, as well as histopathology.[13] Germane to the current results, a recent study incorporated multiple SCI contusion severities and electrophysiological assessments.[18] It was demonstrated that DTI measurements, in terms of relative anisotropy (RA), proximal to the injury epicenter at less than 3 h post-SCI were highly correlated with terminal behavior (BBB and gait assessments) and histopathology at 4 weeks post-injury. Notably, however, MRI-DTI measurements beyond 3 h post-injury were not assessed and critically, RA images resulted in lower signal-to-noise ratios, compared with FA.[34]

The current investigation expanded on these previous studies by implementing high resolution serial MRI-DTI acquisition capable of differentiating injury severities based on FA values over time, which were highly predictive of long-term functional recovery (BBB/gait analysis) and terminal histopathology. In summary, this study demonstrated the extremely powerful utility of measuring early DTI (FA) to distinguish different injury severities and predict long-term functional recovery with high accuracy. This is particularly powerful as it allows one to assess non-invasively the microstructural integrity of the spinal cord *in vivo*.

The contrast between the T2 mapping results and the FA results are noteworthy and suggest greater fidelity of DTI to discretely quantify SCI pathology. This may be due, in part, to the specific properties being assessed by each of the methods. Conventional MRI metrics, such as T2 relaxation times, provide critical information about the content of a given tissue subvolume, whereas DTI provides information about the microstructural boundaries located both within and directly adjacent to a given subvolume. This is particularly important in the context of lesion formation, where the cellular responses may be variable according to injury severity. With discrete lesion foci containing either CSF or hemorrhage, conventional MRI is exceptional at identifying these regions in terms of T2 hyper-intensities or hypo-intensities, respectively. In the severe injury model presented herein, however, these regions frequently became intermixed or dispersed in a fashion such that the net signal for a given volume within the lesion was no longer hyper-intense or hypo-intense. On the contrary, DTI is not susceptible to these complications. Namely, regardless of the specific contents of the lesion (i.e., CSF or blood), the structural boundaries (or lack thereof) affect aqueous diffusion anisotropy equally.

It is noteworthy that diffusion anisotropy maps have provided good gray–white matter contrast in the hyper-acute phase (<6 h post-injury) in previously published studies,[17–19] while in the current study there was little distinction proximal to the injury site at 7 DPI onward. In fact, decreases in the magnitude of diffusion along the spinal cord axis observed by others in the hyperacute phase of SCI[17–19] were reflective of the decreases in diffusion anisotropy (in terms of FA) seen at and beyond 7 DPI in the current study. This suggests that characteristics associated with decreased longitudinal diffusion, such as axonal collapse, are detectable at early time-points, whereas the downstream cyto-architectural breakdown associated with decreases in diffusion anisotropy may require more time to manifest. Further, since FA values effectively did not change from 7 DPI to 28 DPI, this suggests that the majority of microstructural degradation likely occurs beyond the hyperacute phase (i.e., beyond 6 h), but within 7 DPI. Therefore, in contrast to measuring the magnitude of diffusion along the spinal cord axis during the hyperacute phase (< 6 h post-injury), measurements of diffusion anisotropy in the subacute phase (beyond 6 h post-injury) may provide a more stable and discreet method for injury classification and prognosis in SCI models.

For translational research, the comprehensive approach described herein may provide exceptional insight into the temporal dynamics of pharmaceutical or surgical interventions designed to minimize the damage caused by traumatic SCI. Empirical next steps would be to apply this method and employ FA values in humans following acute SCI to potentially predict their long-term functional recovery and to track tissue integrity dynamics over time. This also might promote the creation of a more discrete and objective SCI classification tool, which, in conjunction with the traditional MRI and sensorimotor assessments, may allow practitioners to make more informed decisions regarding planned therapeutic regimens for a patient's long-term care, based on the pathology associated with the subacute condition.

Acknowledgments

Special thanks to Dr. Moriel Vandsburger (University of Kentucky) for providing expert consultation in manuscript preparation and Dr. Richard Kryscio (University of Kentucky) for expert assistance in statistical analysis. This study was supported by National Institutes of Health/National Institute of Neurological Disorders and Stroke (NIH/NINDS) R01NS069633 (A.G.R. and P.G.S.), The Craig H. Neilsen Foundation #260771 (S.P.P.), NIH/NINDS P30 NS051220 and NIH Shared Instrumentation Program Grant S10 1S10RR029541-01.

Author Disclosure Statement

No competing financial interests exist.

References

1. Kirshblum, S.C., Waring, W., Biering-Sorensen, F., Burns, S.P., Johansen, M., Schmidt-Read, M., Donovan, W., Graves, D., Jha, A., Jones, L., Mulcahey, M.J., and Krassioukov, A. (2011). Reference for the 2011 revision of the International Standards for Neurological Classification of Spinal Cord Injury. J. Spinal Cord Med. 34, 547–554.
2. Ditunno, J.F., Little, J.W., Tessler, A., and Burns, A.S. (2004). Spinal shock revisited: a four-phase model. Spinal Cord 42, 383–395.
3. Nishi, R.A., Liu, H., Chu, Y., Hamamura, M., Su, M.Y., Nalcioglu, O., and Anderson, A.J. (2007). Behavioral, histological, and ex vivo magnetic resonance imaging assessment of graded contusion spinal cord injury in mice. J. Neurotrauma 24, 674–689.
4. Simard, J.M., Popovich, P.G., Tsymbalyuk, O., Caridi, J., Gullapalli, R.P., Kilbourne, M.J., and Gerzanich, V. (2013). MRI evidence that glibenclamide reduces acute lesion expansion in a rat model of spinal cord injury. Spinal Cord 51, 823–827.
5. Spanevello, M.D., Tajouri, S.I., Mirciov, C., Kurniawan, N., Pearse, M.J., Fabri, L.J., Owczarek, C.M., Hardy, M.P., Bradford, R.A., Ramunno, M.L., Turnley, A.M., Ruitenberg, M.J., Boyd, A.W., and Bartlett, P.F. (2013). Acute delivery of EphA4-Fc improves functional recovery after contusive spinal cord injury in rats. J. Neurotrauma 30, 1023–1034.
6. Basser, P.J., Mattiello, J., and Lebihan, D. (1994). MR diffusion tensor spectroscopy and imaging. Biophys. J. 66, 259–267.
7. Basser, P.J. (1995). Inferring microstructural features and the physiological state of tissues from diffusion-weighted images. NMR Biomed. 8, 333–344.
8. Beaulieu, C. (2002). The basis of anisotropic water diffusion in the nervous system—a technical review. NMR Biomed. 15, 435–455.
9. Ellingson, B.M., Kurpad, S.N., and Schmit, B.D. (2008). Ex vivo diffusion tensor imaging and quantitative tractography of the rat spinal cord during long-term recovery from moderate spinal contusion. J. Magn. Reson. Imaging 28, 1068–1079.
10. Jirjis, M.B., Kurpad, S.N., and Schmit, B.D. (2013). Ex vivo diffusion tensor imaging of spinal cord injury in rats of varying degrees of severity. J. Neurotrauma 30, 1577–1586.
11. Kozlowski, P., Raj, D., Liu, J., Lam, C., Yung, A.C., and Tetzlaff, W. (2008). Characterizing white matter damage in rat spinal cord with quantitative MRI and histology. J. Neurotrauma 25, 653–676.
12. Fenyes, D.A. and Narayana, P.A. (1999). In vivo diffusion characteristics of rat spinal cord. Magn. Reson. Imaging 17, 717–722.
13. Sundberg, L.M., Herrera, J.J., and Narayana, P.A. (2010). In vivo longitudinal MRI and behavioral studies in experimental spinal cord injury. J. Neurotrauma 27, 1753–1767.
14. Deo, A.A., Grill, R.J., Hasan, K.M., and Narayana, P.A. (2006). In vivo serial diffusion tensor imaging of experimental spinal cord injury. J. Neurosci. Res. 83, 801–810.
15. Kim, J.H., Loy, D.N., Liang, H.F., Trinkaus, K., Schmidt, R.E., and Song, S.K. (2007). Noninvasive diffusion tensor imaging of evolving white matter pathology in a mouse model of acute spinal cord injury. Magn. Reson. Med. 58, 253–260.
16. Ellingson, B.M., Schmit, B.D., and Kurpad, S.N. (2010). Lesion growth and degeneration patterns measured using diffusion tensor 9.4-T magnetic resonance imaging in rat spinal cord injury. J. Neurosurg. Spine 13, 181–192.
17. Kim, J.H., Loy, D.N., Wang, Q., Budde, M.D., Schmidt, R.E., Trinkaus, K., and Song, S.K. (2010). Diffusion tensor imaging at 3 hours after traumatic spinal cord injury predicts long-term locomotor recovery. J. Neurotrauma 27, 587–598.
18. Kim, J.H., Song, S.K., Burke, D.A., and Magnuson, D.S.K. (2012). Comprehensive locomotor outcomes correlate to hyperacute diffusion tensor measures after spinal cord injury in the adult rat. Exp. Neurol. 235, 188–196.
19. Loy, D.N., Kim, J.H., Xie, M., Schmidt, R.E., Trinkaus, K., and Song, S.K. (2007). Diffusion tensor imaging predicts hyperacute spinal cord injury severity. J. Neurotrauma 24, 979–990.
20. Patel, S.P., Sullivan, P.G., Lyttle, T.S., Magnuson, D.S.K., and Rabchevsky, A.G. (2012). Acetyl-l-carnitine treatment following spinal cord injury improves mitochondrial function correlated with remarkable tissue sparing and functional recovery. Neuroscience 210, 296–307.
21. Scheff, S.W., Rabchevsky, A.G., Fugaccia, I., Main, J.A., and Lumpp, J.E. (2003). Experimental modeling of spinal cord injury: characterization of a force-defined injury device. J. Neurotrauma 20, 179–193.
22. Basso, D.M., Beattie, M.S., and Bresnahan, J.C. (1995). A sensitive and reliable locomotor rating scale for open field testing in rats. J. Neurotrauma 12, 1–21.
23. Patel, S.P., Sullivan, P.G., Pandya, J.D., Goldstein, G.A., VanRooyen, J.L., Yonutas, H.M., Eldahan, K.C., Morehouse, J., Magnuson, D.S., and Rabchevsky, A.G. (2014). N-acetylcysteine amide preserves mitochondrial bioenergetics and improves functional recovery following spinal trauma. Exp. Neurol. 257, 95–105.
24. Jenkinson, M., Beckmann, C.F., Behrens, T.E., Woolrich, M.W., and Smith, S.M. (2012). Fsl. NeuroImage 62, 782–790.
25. Rabchevsky, A.G., Fugaccia, I., Sullivan, P.G., Blades, D.A., and Scheff, S.W. (2002). Efficacy of methylprednisolone therapy for the injured rat spinal cord. J. Neurosci. Res. 68, 7–18.
26. Rabchevsky, A.G., Sullivan, P.G., and Scheff, S.W. (2007). Temporal-spatial dynamics in oligodendrocyte and glial progenitor cell numbers throughout ventrolateral white matter following contusion spinal cord injury. Glia 55, 831–843.
27. Rabchevsky, A.G., Sullivan, P.G., Fugaccia, I., and Scheff, S.W. (2003). Creatine diet supplement for spinal cord injury: influences on functional recovery and tissue sparing in rats. J. Neurotrauma 20, 659–669.
28. Ellingson, B.M., Kurpad, S.N., Li, S.J., and Schmit, B.D. (2008). In vivo diffusion tensor imaging of the rat spinal cord at 9.4T. J. Magn. Reson. Imaging 27, 634–642.
29. Mogatadakala, K.V. and Narayana, P.A. (2009). In vivo diffusion tensor imaging of thoracic and cervical rat spinal cord at 7 T. Magn. Reson. Imaging 27, 1236–1241.
30. Leksell, L., Leksell, D., and Schwebel, J. (1985). Stereotaxis and nuclear magnetic-resonance. J. Neurol. Neurosurg. Psychiatry 48, 14–18.
31. Heilbrun, M.P., Sunderland, P.M., McDonald, P.R., Wells, T.H., Cosman, E., and Ganz, E. (1987). Brown-Roberts-Wells stereotactic frame modifications to accomplish magnetic-resonance imaging guidance in 3 planes. Applied Neurophysiol. 50, 143–152.
32. Ellingson, B.M., Ulmer, J.L., and Schmit, B.D. (2008). Morphology and morphometry of human chronic spinal cord injury using diffusion tensor imaging and fuzzy logic. Ann. Biomed. Eng. 36, 224–236.
33. Krzyzak, A.T., Jasinski, A., Kwiecinski, S., Kozlowski, P., and Adamek, D. (2008). Quantitative assessment of injury in rat spinal cords in vivo by MRI of water diffusion tensor. Appl. Magn. Reson. 34, 3–20.
34. Hasan, K.M., Alexander, A.L., and Narayana, P.A. (2004). Does fractional anisotropy have better noise immunity characteristics than relative anisotropy in diffusion tensor MRI? An analytical approach. Magn. Reson. Med. 51, 413–417.

Address correspondence to:
Alexander G. Rabchevsky, PhD
Spinal Cord and Brain Injury Research Center (SCoBIRC)
B471, Biomedical and Biological Sciences Research Building
741 South Limestone Street
Lexington, KY 40536-0509

E-mail: agrab@uky.edu